MODELING MAGNETOHYDRODYNAMICS FLOW OF CONTINUOUS DUSTY PARTICLES IN A NON-NEWTONIAN DARCY FLUID BETWEEN PARALLEL PLATES

Ugwu, U. C.; Olayiwola, R.O.; Adedayo, O. A.; Enefu, P. A.; Akintaro, T. J. & Zhiri. A.B.
Department of Mathematics, Federal University of Technology, Minna, Nigeria.
Email Address: clement.ugwu@futminna.edu.ng **Phone:** 08038450209**.**

Abstract
This paper deals with the study of Magnetohydrodynamics (MHD) flow of continuous dusty particles in a Non-Newtonian Darcy fluid between parallel plates where the lower plate is kept fixed and the upper plate is moving with some velocity. The analytical solutions of the coupled equations were obtained using direct integration and Eigen function expansion techniques after transformation. The resistive forces of Darcy porous medium and the external uniform magnetic field were applied on the flow. The effects of the continuous dusty fluid, non-Newtonian fluid, Darcy model were shown for both the fluid and dust particles. Some results obtained shows that increase in Hartmann number leads to a considerable decrease the velocity of both the fluid phase and that of the particle phase as well as increase in viscosity ratio leads to a slight decrease in the velocity of the fluid but a considerable decrease in the velocity of the particles.

Keywords: Continuous dusty fluid, Eigen function expansion, MHD flow, non-Newtonian Darcy fluid, parallel plates

Introduction
The problem of boundary layer dusty fluid flow has been under investigation over many years ago. The concept of an unsteady flow and heat transfer of a dusty fluid has a wide range of applications in refrigeration, air conditioning, space heating, power generation, chemical processing, pumps, accelerators, nuclear reactors, filtration geothermal systems, and so on. One common example of heat transfer is the radiator in a car, in which the hot radiator fluid is cooled by the flow of air over the radiator surface. On this basis many mathematicians were attracted by this field. The efficiency of these devices is affected by magnetic, Darcy resistance forces and dust particles. The high particle concentration leads to higher particle-phase viscous stresses and can be accounted for endowing the particle phase by the particle-phase viscosity. Datta and Dalal (1995) discussed the flow and heat transfer behavior of dusty fluid over a circular pipe. Unsteady convective flow of a dusty fluid over rectangular channel was discussed by Dalal *et al.* (1998). Bagewadi and Shantharajappa (2000) extended the previous work by considering flow over frenet frame. Ugwu *et al.* (2021a) studied the MHD effects on convective flow of dusty viscous fluid. The problem was solved numerically under the influence of magnetic field.

Similarly, Shawky (2009) studied the unsteady flow of dusty conducting fluid through pipes has been studied analytically and numerically under the influence of transverse magnetic field. Attia (2011) considered the velocities, skin friction factors, and volumetric flow rates are computed and discussed. Madhura and Swetha (2017) studied the influence of volume fraction of dust particles on flow through porous rectangular channel. They used Laplace transform and Finite Difference Method (FDM) to obtain velocities and skin friction factors for fluid as well as dust particles.

Non-Newtonian viscoelastic and temperature-dependent viscosity effects on hydromagnetic dusty fluid flow between parallel plates were studied by Dey (2016). These problems have been solved analytically. In another study, Ghadikolaei *et al.* (2018) applied FDM on the governing equations of the above problem to obtain shear stresses. Ugwu *et al.* (2021b) studied the effects of MHD flow on convective fluids incorporating viscous dissipation energy though it was a Newtonian fluid. This problem was analysed numerically using method of lines and various fluid parameter and that of the particles were obtained.
The aim of this work is to compute the effects of continuous dusty viscous particles and conducting power-law fluid and Darcy resistance force on the velocities and skin friction factors of both fluid phase and

particle phase. A linearization transformation technique is applied on these equations to transform them due to the nonlinear term in the momentum equation.

Formulation of the Problem

The dust particles are assumed to be electrically non-conducting, spherical in shape, and uniformly distributed throughout the fluid. The two plates are assumed to be electrically non-conducting. A constant pressure gradient is applied in the $x-direction$ and a uniform magnetic field (Bo) is applied in the positive $y-direction$. Due to the infinite dimensions in the x and z directions, the physical quantities do not change in these directions, therefore we have $\partial/\partial x = \partial/\partial z = 0$ and the problem becomes unsteady one-dimensional as shown in the figure below.
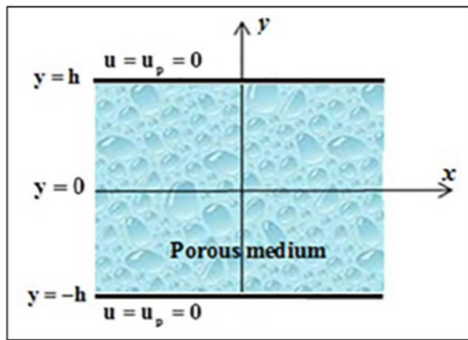

Figure 1: Problem geometry and boundary conditions

Given the governing equations,

$$\rho \frac{\partial u}{\partial t} = -\frac{\partial P}{\partial x} + 2^m \eta (2m+1) \left(\frac{\partial u}{\partial y} \right)^{2m} \left(\frac{\partial^2 u}{\partial y^2} \right) - \left(\sigma \beta_0^2 + \frac{\mu_0}{k_p} \right) u - KN \left(u - u_p \right) \qquad (1)$$

$$\rho_p \frac{\partial u_p}{\partial t} = \mu_p \frac{\partial^2 u_p}{\partial y^2} + KN \left(u - u_p \right) \qquad (2)$$

Subject to,

$$\left. \begin{array}{lll} u(y,0) = \dfrac{y^2}{h}, & u(-h,t) = 0, & u(h,t) = 0 \\[2mm] u_p(y,0) = 0, & u_p(-h,t) = 0, & u_p(h,t) = 0 \end{array} \right\} \qquad (3)$$

Where,

u = velocity of the fluid $\qquad\qquad\qquad\qquad$ σ = electric conductivity of the fluid

u_p = velocity of fluid particles

K= Stokes constant

B_0 = Magnetic field intensity

N = number density of dust particles

Non-Dimensionalisation

Using the following dimensionless variable we non-dimensionalise equation (1) to (3).

$$\hat{x} = \frac{x}{h}; \quad \hat{y} = \frac{y}{h}; \quad \hat{t} = \frac{t\mu_0}{\rho h^2}; \quad \hat{P} = \frac{P\rho h^2}{\mu_0^2}; \quad \hat{u} = \frac{u\rho h}{\mu_0}; \quad \hat{u}_p = \frac{u_p \rho h}{\mu_0}$$

By substitution we have,

$$\frac{\partial u}{\partial t} = \alpha + \frac{1}{R_e} 2^{\frac{n-1}{2}} \eta(n) \left(\frac{\partial u}{\partial y}\right)^{n-1} \left(\frac{\partial^2 u}{\partial y^2}\right) - \left(H_a^2 + S^2\right)u - L_1 Q\left(u - u_p\right) \tag{5}$$

$$\frac{\partial u_p}{\partial t} = \beta \frac{\partial^2 u_p}{\partial y^2} + L_1\left(u - u_p\right) \tag{6}$$

Subject to,

$$\left.\begin{array}{l} u(y,0) = R_e y^2, \quad u(-1,t) = 0, \quad u(1,t) = 0 \\ u_p(y,0) = 0, \quad u_p(-1,t) = 0, \quad u_p(1,t) = 0 \end{array}\right\} \tag{7}$$

Where:

$$\alpha = -\frac{\partial P}{\partial x}, \quad L_1 = \frac{K\rho h^2 N}{\mu_0 \rho_p}, \quad 2m = n-1$$

$$R_e = \left(\frac{\mu_0 \frac{n-2}{n-1}}{\rho h^2}\right)^{n-1}, \quad Q = \frac{\rho_p}{\rho}, \quad S^2 = \frac{h^2}{k_p}, \quad \beta = \frac{\mu_p \rho}{\mu_0 \rho_p}$$

Parameter expansion;

Using parameter expansion technique, we obtain equation (5), (6) and (7)

For $n = 1$; we have:

$$\frac{\partial u}{\partial t} = \alpha + \frac{1}{R_e}\eta\frac{\partial^2 u}{\partial y^2} - \left(H_a^2 + S^2\right)u - L_1Q\left(u - u_p\right) \tag{8}$$

$$\frac{\partial u_p}{\partial t} = \beta\frac{\partial^2 u_p}{\partial y^2} + L_1\left(u - u_p\right) \tag{9}$$

Subject to

$$\left.\begin{array}{lll} u(y,0) = R_e y^2, & u(-1,t) = 0, & u(1,t) = 0 \\ u_p(y,0) = 0, & u_p(-1,t) = 0, & u_p(1,t) = 0 \end{array}\right\} \tag{10}$$

Again, using perturbation techniques, where

$$\left.\begin{array}{l} u = u_0 + Qu_1 + \ldots \\ u_p = u_{p_0} + Qu_{p_1} + \ldots \end{array}\right] \tag{11}$$

Therefore, substituting equation (11) into equation (8), (9) and (10) and collecting like powers of Q, we have that for;

Q^0 :

$$\frac{\partial u_0}{\partial t} = \alpha + \frac{1}{R_e}\eta\frac{\partial^2 u_0}{\partial y^2} - \left(H_a^2 + S^2\right)u_0 \tag{12}$$

$$\frac{\partial u_{p_0}}{\partial t} = \beta\frac{\partial^2 u_{p_0}}{\partial y^2} + L_1\left(u_0 - u_{p_0}\right) \tag{13}$$

Subject to

$$\left.\begin{array}{lll} u_0(y,0) = R_e y^2, & u_o(-1,t) = 0, & u_0(1,t) = 0 \\ u_{p_0}(y,0) = 0, & u_{p_0}(-1,t) = 0, & u_{p_0}(1,t) = 0 \end{array}\right\} \tag{14}$$

Q^1 :

$$\frac{\partial u_1}{\partial t} = \frac{1}{R_e}\eta\frac{\partial^2 u_1}{\partial y^2} - \left(H_a^2 + S^2\right)u_1 - L_1\left(u_0 - u_{p_0}\right) \tag{15}$$

$$\frac{\partial u_{p_1}}{\partial t} = \beta\frac{\partial^2 u_{p_1}}{\partial y^2} + L_1\left(u_1 - u_{p_1}\right) \tag{16}$$

Subject to

$$\left.\begin{array}{l} u_1\left(y,0\right) = 0, \quad u_1\left(-1,t\right) = 0, \quad u_1\left(1,t\right) = 0 \\[6pt] u_{p_1}\left(y,0\right) = 0, \qquad u_{p_1}\left(-1,t\right) = 0, \quad u_{p_1}\left(1,t\right) = 0 \end{array}\right\} \tag{17}$$

Transformation
Since the boundary conditions are from -1 to 1, we wish to transform it to 0 to 1; thus let,
$$x = \frac{y+1}{2} \tag{18}$$

Applying (18) into equation (12) to (17), we obtain

$$\frac{\partial u_0}{\partial t} = \alpha + \frac{\eta}{4R_e}\frac{\partial^2 u_0}{\partial x^2} - \left(H_a^2 + S^2\right)u_0 \tag{19}$$

$$\frac{\partial u_{p_0}}{\partial t} = \frac{\beta}{4}\frac{\partial^2 u_{p_0}}{\partial x^2} + L_1\left(u_0 - u_{p_0}\right) \tag{20}$$

$$\frac{\partial u_1}{\partial t} = \frac{\eta}{4R_e}\frac{\partial^2 u_1}{\partial x^2} - \left(H_a^2 + S^2\right)u_1 - L_1\left(u_0 - u_{p_0}\right) \tag{21}$$

$$\frac{\partial u_{p_1}}{\partial t} = \frac{\beta}{4}\frac{\partial^2 u_{p_1}}{\partial x^2} + L_1\left(u_1 - u_{p_1}\right) \tag{22}$$

Subject to,

$$
\left.\begin{array}{lll}
u_0(y,0) = R_e\left(4x^2 - 4x + 1\right), & u_o(-1,t) = 0, & u_0(1,t) = 0 \\
u_{p_0}(y,0) = 0, & u_{p_0}(-1,t) = 0, & u_{p_0}(1,t) = 0 \\
u_1(y,0) = 0, & u_1(-1,t) = 0, & u_1(1,t) = 0 \\
u_{p_1}(y,0) = 0, & u_{p_1}(-1,t) = 0, & u_{p_1}(1,t) = 0
\end{array}\right\}
\qquad (23)
$$

Analytical solution

Using Eigen-function expansion techniques, we obtain the solution to equation (19)- (22) as follows;

$$
u_0(x,t) = \sum_{n=1}^{\infty}\left(A_4 e^{Bt} - A_3\right)\sin(n\pi)x; \qquad (24)
$$

$$
u_{P_0}(x,t) = \sum_{n=1}^{\infty}\sum_{n=1}^{\infty}\left[A_7\left(e^{B_2} - 1\right) + A_8\left(e^{-B_1} - 1\right)\right]e^{B_1 t}\sin(n\pi)x \qquad (25)
$$

$$
u_1(x,t) = \sum_{n=1}^{\infty}\left\{\sum_{n=1}^{\infty}\sum_{n=1}^{\infty}A_{18}e^{B_3 t}\right\}\sin(n\pi)x \qquad (26)
$$

$$
u_{p1}(x,t) = \sum_{n=1}^{\infty}\left\{\sum_{n=1}^{\infty}\sum_{n=1}^{\infty}\sum_{n=1}^{\infty}A_{20}e^{B_6 t}\right\}\sin(n\pi)x ; \qquad (27)
$$

Where,

$$A_1 = 2R_e \left(\frac{8}{n^3\pi^3} - \frac{1}{n\pi} \right) \left\{ (-1)^n - 1 \right\} ; A_4 = A_3 + A_1 ; A_9 = A_7 \left(e^{B_2} - 1 \right) + A_8 \left(e^{-B_1} - 1 \right)$$

$$A_2 = \frac{2\alpha}{n\pi} \left[1 - (-1)^n \right] \qquad A_3 = \frac{A_2}{B} \quad \begin{aligned} A_7 &= L_1 A_5 \\ A_8 &= L_1 A_6 \end{aligned} \quad B_3 = e^{\left(-A - \frac{\eta}{4R_e}(n\pi)^2 \right)}$$

$$B = \left(-A - \frac{\eta}{4R_e}(n\pi)^2 \right) A_5 = \frac{A_4}{B_2}, \quad A_6 = \frac{A_3}{B_1} \quad B_2 = B - B_1 \quad A_{18} = A_{16} - A_{17}$$

$$A_{10} = \frac{2L_1}{n\pi} A_9, \quad A_{12} = \frac{2L_1}{n\pi} A_3, \quad A_{11} = \frac{2L_1}{n\pi} A_4 \quad B_4 = B_1 - B_3; \qquad B_5 = B - B_3 \qquad (28)$$

$$A_{13} = \frac{A_{10}}{B_4}; \quad A_{14} = \frac{A_{11}}{B_5}; \quad A_{15} = \frac{A_{12}}{B_3}; \quad \begin{aligned} A_{16} &= A_{13} \left(e^{B_4} - 1 \right) \\ A_{17} &= A_{14} \left(e^{B_5} - 1 \right) + A_{15} \left(e^{-B_3} - 1 \right) \end{aligned}$$

$$B_7 = B_3 - B_6; \quad A_{19} = \frac{A_{18}}{B_7}, \quad A_{20} = L_1 A_{19} \left(e^{B_7} - 1 \right)$$

Results and Discussion

The coupled differential Equation (12) - (16) with respect to the boundary conditions (14) and (17) are solved analytically using Eigen function expansion techniques. For numerical results and graphically representation, we considered :

Re = 1, L_1 = 0.1, β = 1, Ha = 0.1, S = 1, η = 1, α = 1, Q = 0.5, n = 1, t = 1:

These values are kept as common in entire study except the varied values as displayed in the respective figures. The results obtained show the influences of the non-dimensional governing parameters, namely Reynold number parameter (Re), Hartmann number (Ha), Pressure gradient (α), viscosity ratio (β), time (t), for both the fluid flow and particles.

Figs. 2 and 3 depicts the effects of Reynold number on both the fluid flow and the particles. It shows that increase in Reynold number leads to an increase in both the fluid flow and that of the particles. This is because Reynolds number helps to predict flow pattern in different situation, thus increase in the Reynold number leads to a more turbulent flow which increases both the velocity of the fluid and that of the particles.

Figs. 4 and 5 depicts the effects of Hartmann number on both the fluid flow and the particles. Its shows that increase in Hartmann number leads to a considerable decrease the velocity of both the fluid phase and that

of the particle phase. This is because of its resistive effect but the fluid phase reaches its steady state faster than the particle phase.

Figs 6 and 7 depicts the effect of pressure gradient on both the fluid phase and particle phase. Its shows that increase in pressure with time leads to an increase in the velocity of the fluid phase and the velocity of the particle phase.

Figs. 8 and 9 depicts the effects of viscosity ratio on both the fluid phase and the particle phase. It shows that increase in viscosity ratio leads to a slight decrease in the velocity of the fluid but a considerable decrease in the velocity of the particles. This is because the particle phase is influenced more than the fluid phase. Viscosity ratio is the main parameter than governs the dusty particle motion.

Figs. 10 and 11 depicts the effect of time on both the fluid phase and the particle phase. It shows that an increase in time leads to an increase in both the fluid phase and particle phase. This is because with time, heat is been generated which reduces the Lorentz force.

Figs. 12 and 13 depicts the effect of the power law index. It is observed that increasing the index, n there is little or no change in velocity profiles of both the fluid phase and particle phase.
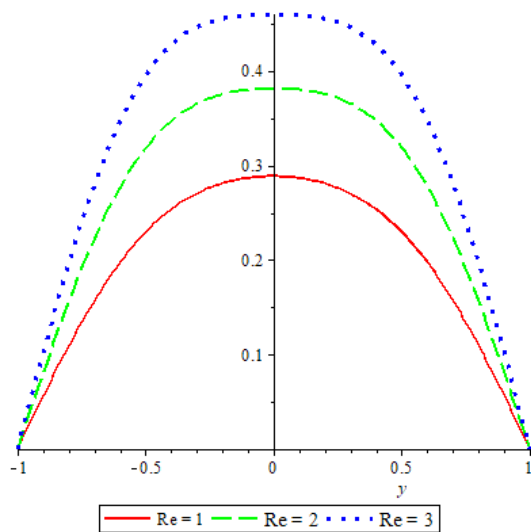
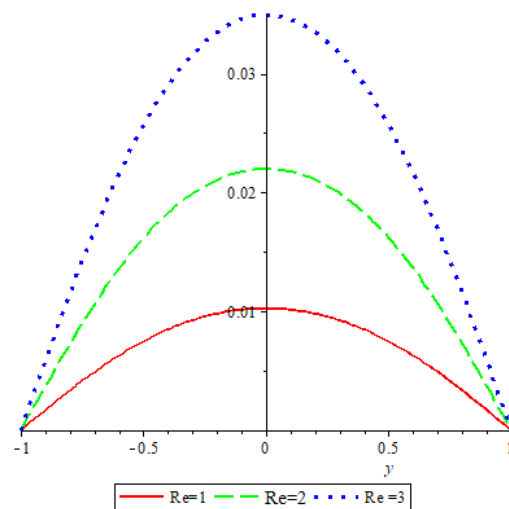Figure.2: Effects of Reynoid number on the fluid phase.

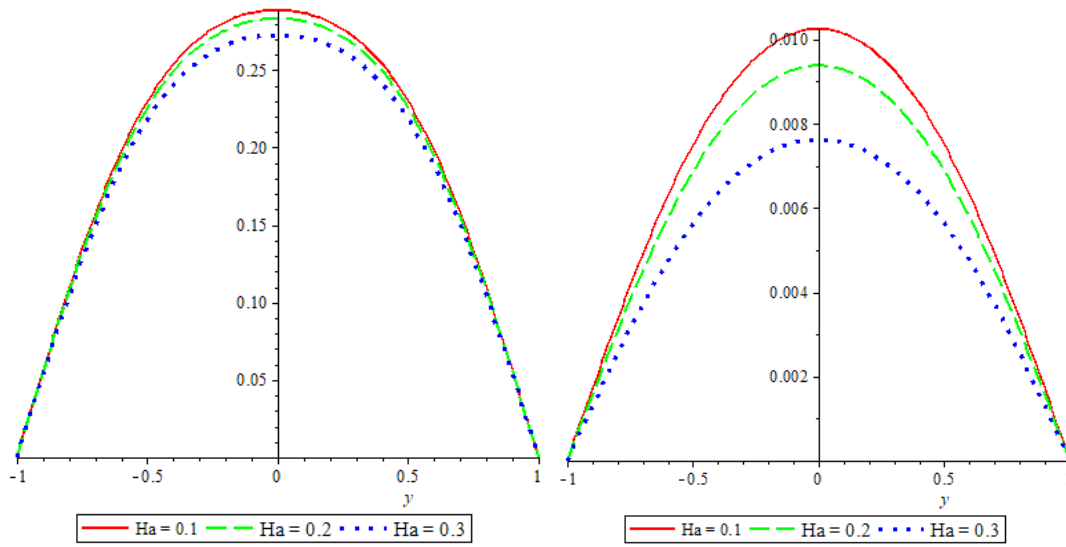Figure.3: Effects of Reynoid number on the particle phase.

Figure.4: Effects of Hartmann number on the fluid phase. [Ha = 0.1, 0.3, 0.5 for Red, Green, Blue]

Figure.5: Effects of Hartmann number on the particle phase. [Ha = 0.1, 0.3, 0.5 for Red, Green, Blue]
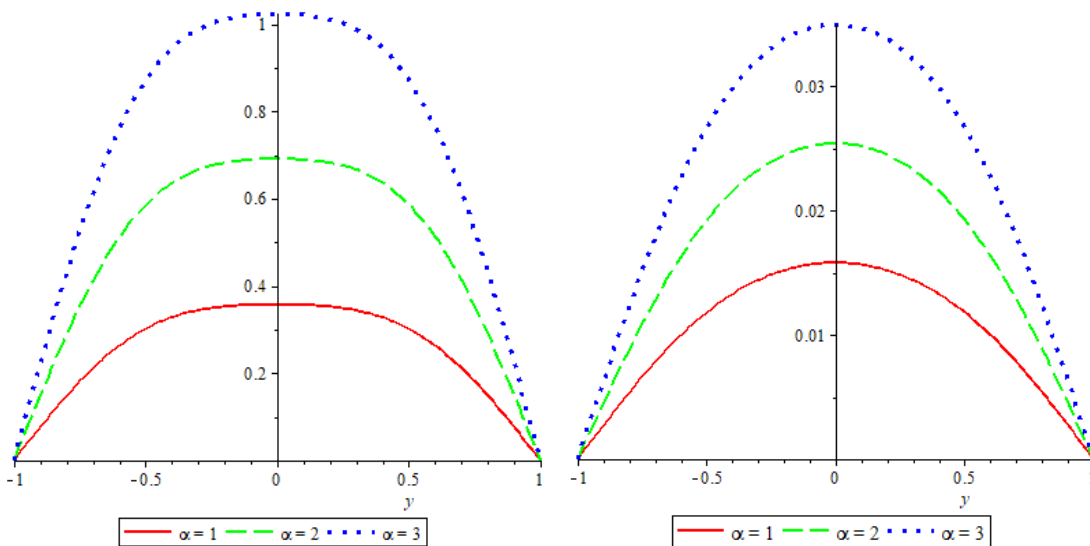

Figure.6: Effects of pressure gradient on the fluid phase.

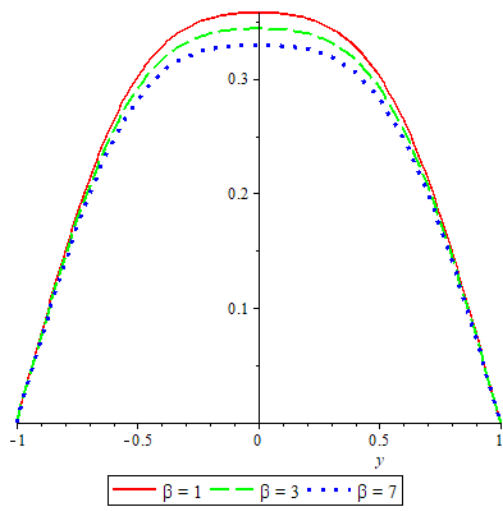Figure.7: Effects of pressure gradient on the particle phase.

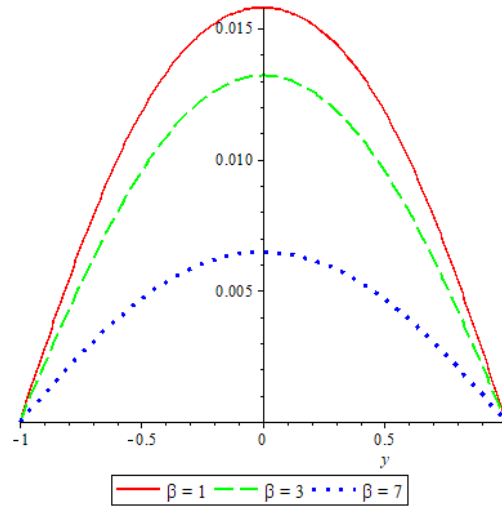Figure.8: Effects of viscosity ratio on the fluid phase.

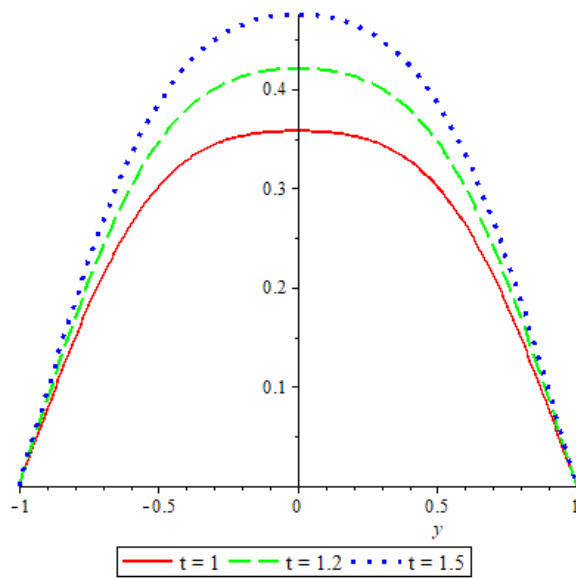Figure.9: Effects of viscosity ratio on the particle phase.

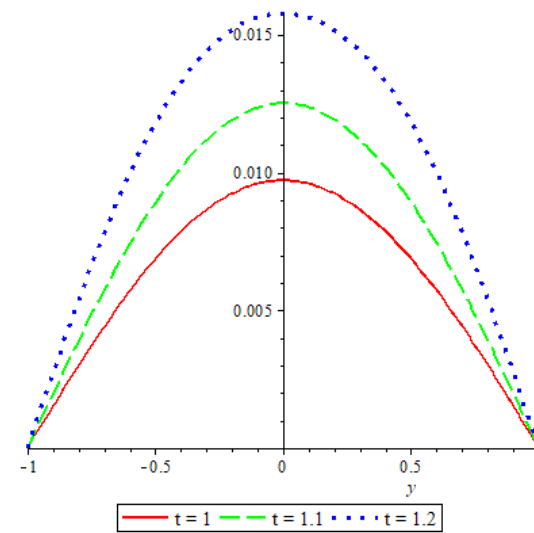Figure.10: Effects of time on the fluid phase.

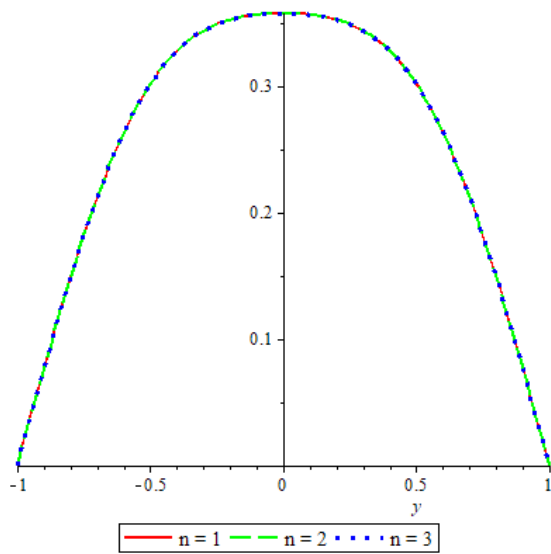

Figure.11: Effects of time on the particle phase.

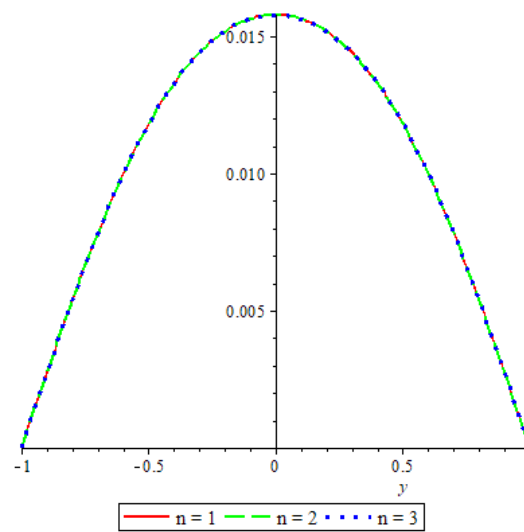Figure.12: Effects of power law index on the fluid phase.

Figure.13: Effects of power law index on the particle phase.

Conclusion

This paper presents the continuous dusty viscous particle model and non-Newtonian power law fluid flow. The conducting fluid was studied considering magnetic and Darcy resistance forces. The governing mathematical equations were solved analytically using Eigen function expansion techniques and were analyses using MAPLE software. The effects of some governing parameters on the flow are presented graphically and discussed. The findings are summarized as follows;

1. Increase in Reynold number leads to an increase in both the fluid flow and that of the particles.
2. Increase in Hartmann number leads to a considerable decrease the velocity of both the fluid phase and that of the particle phase.
3. Increase in pressure with time leads to an increase in the velocity of the fluid phase and the velocity of the particle phase.
4. Increase in viscosity ratio leads to a slight decrease in the velocity of the fluid but a considerable decrease in the velocity of the particles.
5. Increase in time leads to an increase in both the fluid phase and particle phase.
6. Increasing the index, n there is little or no change in velocity profiles of both the fluid phase and particle phase.

Refereences

Attia, H. A. (2011) Transient circular pipe MHD flow of a of a dusty fluid considering hall effect. *Kragujevac Journal of Science,* 23, 15–23

Begewadi, C. S., & Shantharajappa, A. N. (2000). A study of unsteady dusty gas flow in frenet frame field. *Industrial Journal of Pure and Applied Math*, 31, 14–20.

Dalal, D.C., Datta, N., & Mukherjea, S. K. (1998). Unsteady natural convection of a dusty fluid in an infinite rectangular channel. *International Journal of Heat Mass Transfer*, 41(3), 547–62.

Datta, N., & Dalal, D.C. (1995). Pulsatile flow of heat transfer of a dusty fluid through an infinitely long annular pipe. *International Journal of Multiphase Flow,* 21(3), 515–28.

Dey, D. (2016). Non-Newtonian effect on hydromagnetic dusty stratified fluid flow through a porous medium with volume fraction. *Proceedings of the National Academy of Sciences*, (A) 86: 47–56.

Ghadikolaei, S.S., Hosseinzadeh, K. H., & Ganji, D. D. (2018). Fe3O4–(CH2OH)2 Nano fluid analysis in a porous medium under MHD radiative boundary layer and dusty fluid. *Journal of Molecular Liquid*, 258, 172–185.

Madhura, K. R., & Swetha, D. S. (2017). Influence of volume fraction of dust particles on flow through porous rectangular channel. *International Journal of Math Trends Technology*, 50, 261–275.

Shawky, H. M. (2009). Pulsatile flow with heat transfer of dusty magnetohydrodynamic Ree-Eyring fluid through a channel. *Heat Mass Transfer*, 45,1261–1269

Ugwu, U. C., Cole, A. T., & Olayiwola, R. O. (2021a). Analysis of Magnetohydrodynamics effects on convective flow of dusty viscous fluid. *Science World Journal*,16 (2) , 85-89.

Ugwu, U. C., Cole, A. T., Olayiwola, R. O. & Kazeem, J. A. (2021b) Method of Lines Analysis of Mhd Effect on Convectve Flow of Dusty Fluid In The Presence of Viscous Energy Dissipation. Journal *of Science, Technology, Mathematics and Education (JOSTMED)*, 17(1), 140-151.